Proc. Natl. Acad. Sci. USA
Vol. 89, pp. 10940–10944, November 1992
Biochemistry

Predicted α-helical regions of the prion protein when synthesized as peptides form amyloid

(scrapie/β-sheet/protein secondary structure/amyloid fibrils)

MARIA GASSET*, MICHAEL A. BALDWIN*, DAVID H. LLOYD†, JEAN-MARC GABRIEL*, DAVID M. HOLTZMAN*, FRED COHEN‡§, ROBERT FLETTERICK§¶, AND STANLEY B. PRUSINER*¶‖

Departments of *Neurology, ¶Biochemistry and Biophysics, ‡Medicine, and §Pharmaceutical Chemistry, University of California, San Francisco, CA 94143; and †Applied Biosystems Inc., Foster City, CA 94404

Contributed by Stanley B. Prusiner, July 22, 1992

ABSTRACT **By comparing the amino acid sequences of 11 mammalian and 1 avian prion proteins (PrP), structural analyses predicted four α-helical regions. Peptides corresponding to these regions of Syrian hamster PrP were synthesized, and, contrary to predictions, three of the four spontaneously formed amyloids as shown by electron microscopy and Congo red staining. By IR spectroscopy, these amyloid peptides exhibited secondary structures composed largely of β-sheets. The first of the predicted helices is the 14-amino acid peptide corresponding to residues 109–122; this peptide and the overlapping 15-residue sequence 113–127 both form amyloid. The most highly amyloidogenic peptide is AGAAAAGA, which corresponds to Syrian hamster PrP residues 113–120 and is conserved across all species for which the PrP sequence has been determined. Two other predicted α-helices corresponding to residues 178–191 and 202–218 form amyloids and exhibit considerable β-sheet structure when synthesized as peptides. These findings suggest the possibility that the conversion of the cellular isoform of PrP to the scrapie isoform of PrP involves the transition of one or more putative PrP α-helices into β-sheets and that prion diseases are disorders of protein conformation.**

Infectious prion particles are composed largely, if not entirely, of the scrapie isoform of the prion protein (PrP^{Sc}) (1). PrP^{Sc} is produced from the cellular isoform of the prion protein (PrP^{C}) by a posttranslational process that probably occurs in the endocytic pathway (2–4). In cultured cells and probably brain, PrP^{Sc} accumulates in lysosomes (5–9). Limited proteolysis of PrP^{Sc} generates a peptide of 27–30 kDa (PrP 27–30) by removal of the N-terminal ≈67 amino acids; the resulting protease-resistant core is encoded by codons 90–231 (10, 11). Generation of PrP 27–30 in the presence of detergent produces rod-shaped particles that are indistinguishable from many other amyloids based on their ultrastructural morphology and tinctorial properties (12, 13). In the brains of humans and animals with prion diseases, sometimes PrP^{Sc} accumulates in the extracellular space as amyloid plaques (14). These plaques, like the polymers of PrP 27–30, stain with Congo red dye and show green-gold birefringence when viewed by polarization microscopy (15, 16). All known amyloids are composed of protein polymers, the secondary structures of which exhibit extensive β-pleated sheets (17). From the amino acid sequence of mammalian PrP, we predicted regions of β-sheets (18), and recent IR spectroscopy studies confirm the presence of β-sheet structures within polymers of PrP 27–30 (19, 20).

In the study reported here, we synthesized peptides homologous to portions of the Syrian hamster (SHa) PrP sequence and examined their physical characteristics by attenuated total reflection (ATR) Fourier transform IR spectroscopy (FTIR) (21). The particular peptides were chosen based on structural predictions where the PrP amino acid sequences from 11 mammalian and 1 avian sources were compared (22). Those analyses suggested the possibility that PrP might fold into a monomeric molecule with four α-helices (ref. 23; J.-M.G., F.C., R.F., and S.B.P., unpublished results). Unexpectedly, synthetic peptides corresponding to three of the four putative α-helices exhibit extensive β-sheet structure as well as the ultrastructural and tinctorial properties of amyloid.

MATERIALS AND METHODS

All PrP peptides (Table 1) were assembled by using the 9-fluorenylmethoxycarbonyl variant of the Merrifield solid-phase method on an Applied Biosystems model 432A Synergy peptide synthesizer. Peptides with side-chain protection were cleaved from the resins by using thioanisole/ethanedithiol/trifluoroacetic acid (TFA) and precipitated with *tert*-butyl methyl ether. They were pelleted by centrifugation, suspended in ether, washed three times, repelleted, dissolved in water/isopropanol, and filtered. Peptides without side-chain protection were cleaved with 90% (vol/vol) TFA. The solutions were lyophilized, and the peptides were analyzed by reversed-phase HPLC and plasma desorption mass spectrometry. The majority of peptides were >80% pure and were used without further purification. The initial product for peptide H4 was ≈20% pure, and it was purified by preparative HPLC and reanalyzed. The synthesis of SHaPrP-(113–120) gave 40% Ala_6Gly_2 (the desired product) and 60% Ala_5Gly_2, which could not be separated by HPLC. Solutions of the peptides were prepared in 1,1,1,3,3,3-hexafluoroisopropyl alcohol (HFIP; Aldrich) and their concentrations were determined by amino acid analysis by hydrolyzing aliquots at 110°C *in vacuo* for 24 hr in the presence of 6 M HCl and phenol, preparing orthofluorophthaldehyde derivatives, and analyzing by HPLC with fluorometric detection (11). The Alzheimer peptide βA4-(1–28) was supplied by Peninsula Laboratories.

After quantitation of each solution, aliquots were taken, the solvent was evaporated, and the peptides were further dried *in vacuo* before dispersion in measured volumes of an appropriate solvent, either 20 mM Hepes (pH 7.4) or HFIP. Samples that were dispersed in phospholipids were sonicated five times for 2 min each. Similar treatment of the peptides in the absence of phospholipids had no observable effects. Prion

The publication costs of this article were defrayed in part by page charge payment. This article must therefore be hereby marked "*advertisement*" in accordance with 18 U.S.C. §1734 solely to indicate this fact.

Abbreviations: PrP, prion protein; PrP^{C}, cellular isoform of the prion protein; PrP^{Sc}, scrapie isoform of the prion protein; SHa, Syrian hamster; LF-β, low frequency β; HFIP, 1,1,1,3,3,3-hexafluoroisopropyl alcohol; ATR, attenuated total reflection; FTIR, Fourier transform infrared spectroscopy; TFA, trifluoroacetic acid.

‖To whom reprint requests should be addressed at: Department of Neurology, HSE-781, University of California, San Francisco, CA 94143-0518.

Table 1. Peptides used in this study

Peptide	Sequence	% LF-β	EM	Congo red
H1	Ac-MKHMAGAAAAGAVV-NH_2	60	+	+
H2	Ac-MLGSAMSRPMMHF-NH_2	23	−	−
H3	Ac-DCVNITIKQHTVTT-NH_2	55	+	+
H4	Ac-DIKIMERVVEQMCTTQY-NH_2	70	+	+
SHaPrP-(113–120)	AGAAAAGA	80	+	+
SHaPrP-(113–127)	AGAAAAGAVVGGLGG	70	+	+
SHaPrP-(121–136)	Ac-VVGGLGGYMLGSAMSR	14	−	−
βA4-(1–28)	DAEFRHDSGYEVHHQKLVFF-AEDVGSNK	45	+	+

The % LF-β values were calculated from self-deconvoluted ATR-FTIR spectra of peptide films deposited from 20 mM Hepes (pH 7.4) and subjected to hydrogen/deuterium exchange. EM refers to the observation of fibrils by electron microscopy. Congo red refers to the observation of green-gold birefringence by polarized microscopy. Ac, acetyl.

rods were prepared by discontinuous sucrose gradient ultracentrifugation (13).

ATR-FTIR was carried out using a Laser Precision analytical model RFX-30 FTIR spectrophotometer equipped with a liquid N_2-cooled mercury cadmium telluride (MCT) detector. The instrument was continuously purged with N_2. The internal reflection element was a germanium ATR plate (50 × 20 × 2 mm) with an aperture angle of 45° yielding 25 internal reflections. Samples were prepared by drying the peptide dispersion (typically 80 μl of a 1 μg/μl solution) on the surface of the ATR element under N_2 at room temperature. Exchange of labile hydrogen by deuterium (necessary for distinguishing α-helix from random coil) was achieved by flushing with ^2H_2O-saturated N_2 for 2 hr. For each sample, 150 scans were averaged at a resolution of 2 cm^{-1}. Analysis of the amide I′ band (1700–1600 cm^{-1}) was performed as described by Goormaghtigh *et al.* (21).

Electron microscopy was carried out by using specimen grids that were coated with 0.25% Formvar and then carbon and subjected to glow discharge (13). Five microliters of 0.5–2.5 μM peptide suspension was applied to a grid for 1 min before any excess was washed away. Negative staining was performed in uranyl formate for 10 sec (25, 26). Specimen grids were examined by using a JEOL 100CX electron microscope at 80 keV (1 eV = 1.602 × 10^{-19} J).

Aliquots of each peptide suspension were air dried on glass slides, dehydrated for 5 min with 80% ethanol, and stained for 20 min with 5% Congo red prepared in 80% ethanol saturated with NaCl (13). Excess Congo red was removed by washing with 90% ethanol. The stained samples were examined for green-gold birefringence using an Orthoplan Leitz microscope equipped with strain-free lenses, optimally aligned cross-polarizers, and a 100-W quartz-halide light source.

RESULTS

Synthetic Peptides. By comparing the 11 mammalian and 1 avian PrP sequences, four regions were identified that might form α-helices under monomeric conditions, which we designated H1, H2, H3, and H4 corresponding to residues 109–122, 129–140, 178–191, and 202–218, respectively (Fig. 1) (ref. 23; J.-M.G., F.C., R.F., and S.B.P., unpublished results). If the putative helices were to exist, then PrP might fold into a four-helix bundle domain. Most of peptide H1 overlaps with the putative transmembrane helix (27); the C-terminal two-thirds of H1 is conserved across all species examined to date (22). H2 also partially overlaps with the previously predicted transmembrane helix. H3 contains what was previously predicted to be a β-sheet (18). H4 overlaps with the previously predicted second α-helix (27). To minimize changes to the hydrophobicity, the majority of the PrP peptides were synthesized with acetyl and amide groups at their N and C termini, respectively.

ATR-FTIR. Of the four putative helical peptides H1–H4, only the most weakly predicted helix, H2, proved to be readily soluble in water. In contrast, H1 was highly insoluble, whereas H3 and H4 displayed limited solubility in water. The ATR-FTIR spectra of the amide I′ bands for hydrated peptide films are shown in Fig. 2*A*. The IR spectrum of H1 (Fig. 2*A*, spectrum i) has an amide I′ band with a maximum absorbance at 1621 cm^{-1}, which is characteristic of a β-pleated sheet maintained by very strong hydrogen bonds. The unusually low frequency of this absorption maximum and the presence of a residual amide II band after 2 hr of hydrogen/deuterium exchange confirm the existence of intermolecular interactions. We have classified this absorption as resulting from a low-frequency β (LF-β) sheet. H2 gave a different spectrum with a maximum absorbance at 1655 cm^{-1}, which is characteristic of multiple-ordered structures including α-helix, β-sheet, and turns with little indication of any LF-β sheet (Fig. 2*A*, spectrum ii). The ATR-FTIR spectra of H3 and H4 (Fig. 2*A*, spectra iii and iv) indicate that the former contains a mixture of LF-β and turns, whereas H4 is predominantly LF-β. Any residual TFA remaining from the synthesis of H3 would absorb at 1670 cm^{-1} and could be confused with turns. Since H3 contains no arginine, the clean-up procedures employed should have been sufficient to remove TFA; furthermore, no other peptides showed significant peaks with a maximum absorbance at this frequency even though some of them contained arginine, which has a strong affinity for TFA. The percentages of LF-β sheet for each peptide as calculated by self-deconvolution (Table 1) often underestimate the LF-β sheet for structures having a high degree of β-sheet and overestimate it for those with little or none.

To identify the region of the H1 peptide involved in amyloid formation, we synthesized peptides corresponding to residues 113–127 and 113–120; both peptides displayed a LF-β sheet structure (Fig. 2*B*, spectra ii and iii). The peptide SHaPrP-(121–136), which links the C-terminal portion of the conserved region with H2, gave an ATR-FTIR spectrum indicative of mixed structures, mainly α-helical (Fig. 2*B*, spectrum i). These findings argue that the octapeptide AGAAAAGA is sufficient for β-sheet association, whereas the C-terminal portion of the conserved region VVGGLGG is

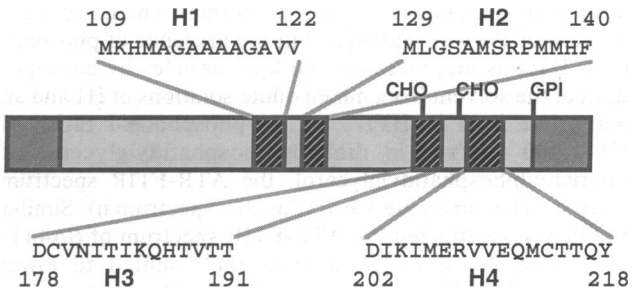

FIG. 1. Schematic representation of SHaPrP showing the four proposed α-helices H1–H4 (boxed regions with diagonal lines). One-letter amino acid code shows the sequences of the synthetic peptides corresponding to the proposed helices; codon numbers for the PrP open reading frame, which encodes a protein of 254 amino acids, are given for the first and last residue of each peptide. A signal peptide of 22 residues is cleaved from the N terminus, and a peptide of 23 residues is removed from the C terminus when the glycosylinositol phospholipid (GPI) anchor is added (shaded boxes at each end). Asn-linked carbohydrates (CHO) are added to residues 181 and 197.

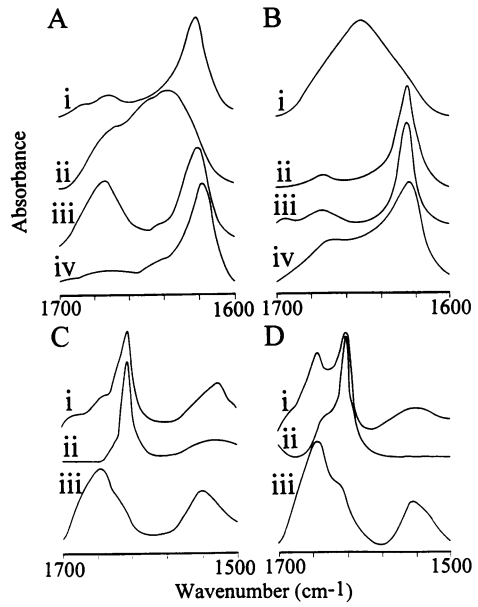

FIG. 2. (*A* and *B*) Amide I region of the ATR-FTIR spectra of peptide films deposited from 20 mM Hepes (pH 7.4) and exchanged with ^2H_2O-saturated N_2 for 2 hr. (*A*) Spectrum i, H1; spectrum ii, H2; spectrum iii, H3; spectrum iv, H4. (*B*) Spectrum i, SHaPrP-(121–136); spectrum ii, SHaPrP-(113–127); spectrum iii, SHaPrP-(113–120); spectrum iv, βA4-(1–28). (*C* and *D*) Effects of environmental conditions on the 1700- to 1500-cm^{-1} region of the ATR-FTIR spectra of H1 (*C*) and βA4-(1–28) (*D*). Spectra i, in the presence of $NaDodSO_4$ (10% final concentration) and hydrogen/deuterium exchanged; spectra ii, dispersed 1:25 (wt/wt) in dimyristylphosphatidylglycerol, sonicated five times for 2 min, and hydrogen/deuterium exchanged; spectra iii, deposited from HFIP without rehydration. The preparation of the samples and the analysis of the data are described in *Materials and Methods*.

not amyloidogenic. As a control we measured the FTIR spectrum of the Alzheimer peptide βA4-(1–28) (Fig. 2*B*, spectrum iv), which has been shown by IR spectroscopy to have a β-sheet structure (28).

The secondary structure of peptides can be affected by the choice of buffer, salt, pH, detergent, solvent, and temperature as illustrated in Fig. 2 *C* and *D* for amide I and amide II bands of the ATR-FTIR spectra of H1 and βA4-(1–28). The presence of $NaDodSO_4$ had little effect on the IR absorption of H1, even at $NaDodSO_4$ concentrations up to 10% (Fig. 2*C*, spectrum i), whereas the β-sheet structure of βA4-(1–28) was significantly disrupted (Fig. 2*D*, spectrum i). The LF-β sheet structure of H1 was maximized in the presence of phospholipids. H1 was incorporated into lipid vesicles by coevaporation of the solvent from mixed dilute solutions of H1 and an appropriate lipid in HFIP. At H1/phospholipid ratios of 1:25–1:100 (wt/wt) in dioleolylphosphatidylglycerol or dimyristoylphosphatidylglycerol, the ATR-FTIR spectrum changed to become pure LF-β (Fig. 2*C*, spectrum ii). Similar treatment also affected the ATR-FTIR spectrum of βA4-(1–28) in that the shoulder at 1670 cm^{-1} shifted to lower frequency (Fig. 2*D*, spectrum ii). When H1 was deposited directly from HFIP solution, it showed a different amide I′ maximum at 1656 cm^{-1} (Fig. 2*C*, iii). When treated with ^2H_2O to differentiate between α-helix and random coil, a rapid change was observed in the IR spectrum, which within 1 min became indistinguishable from that shown in Fig. 2*A*, spectrum i, characteristic of aqueous media. Identical behavior was shown by βA4-(1–28) (Fig. 2*D*, spectrum iii). Unlike the βA4 peptides that were reported to lose amyloid structure at high or low pH, the spectrum of H1 showed no pH dependence (data not shown).

Electron Microscopy. The LF-β sheet exhibited by H1, H3, H4, and some of the other synthetic peptides suggested that these might participate in forming intermolecular clusters or aggregates. Electron microscopy of H1 revealed clusters of fibrils deposited from suspension in 20 mM Hepes at pH 7.4 (Fig. 3*A*). The fibrils showed a tendency for lateral association and were stable over the pH range studied (i.e., 2.5–7.4). H1 fibers were generally uniform in size with diameters of ≈6 nm, but it is not certain whether each is a single fibril because some of the fibers illustrated in Fig. 3 *B–D* and *F* for other peptides are clearly double or multiple fibrils. Fibril formation was observed for SHaPrP-(113–127) (Fig. 3*B*), H3 (Fig. 3*C*), H4 (Fig. 3*D*), and SHaPrP-(113–120) (data not shown); all of these peptides were shown by ATR-FTIR to have LF-β structure. Peptides H2 and SHaPrP-(121–136) for which ATR-FTIR indicated no LF-β sheet showed no fibril formation, even at concentrations substantially greater than that at which H1 readily formed fibrils. For comparison, electron micrographs of infectious prion rods composed largely of PrP 27–30 isolated from scrapie-infected hamster brain by discontinuous sucrose gradient ultracentrifugation (Fig. 3*E*) as well as synthetic βA4-(1–28) fibrils (Fig. 3*F*) are shown, both of which have been reported (13, 29).

Congo Red Birefringence. To determine if the synthetic PrP peptides exhibited the same tinctorial properties of amyloid as the prion rods, they were stained with Congo red dye. Those peptides displaying the characteristic low-frequency bands in their ATR-FTIR spectra and fibrils by electron microscopy also exhibited green-gold birefringence when stained with Congo red dye and viewed by cross-polarization microscopy. Results similar to those depicted for H1 (Fig. 4) were obtained for H3, H4, SHaPrP-(113–120), SHaPrP-(113–127), and PrP 27–30 (data not shown). As expected from the ATR-FTIR spectra, neither H2 nor SHaPrP-(121–136) exhibited this phenomenon.

DISCUSSION

Three regions of the SHaPrP sequence were identified that when synthesized as isolated peptides were insoluble in water and formed amyloid fibrils. These findings raise the possibility that the synthesis of PrP^{Sc} may involve the conversion of α-helical regions of PrP^{C} into β-sheets. This proposed mechanism is consistent with the insolubility of PrP^{Sc} (30), the protease resistance of PrP^{Sc} (31), the propensity of PrP 27–30 to polymerize in amyloid (12, 13), and the increase in antigenicity of PrP^{Sc} after denaturation (32, 33). In contrast to PrP^{Sc}, PrP^{C} is soluble in nondenaturing detergents, is readily hydrolyzed by proteases, and does not form polymers, and its antigenicity is not increased by denaturation. All three of the putative α-helices that undergo β-sheet formation are contained within the region of PrP^{Sc} that is protease resistant, designated PrP 27–30. In Gerstmann–Sträussler–Scheinker disease with neurofibrillary tangles (34), a truncated form of PrP (residues 58–150) has been found to be the major protein within amyloid plaques (35). This truncated PrP molecule contains only the H1 domain, which seems sufficient for amyloid formation, especially in view of the results with synthetic H1 peptides reported here. In Alzheimer disease, β-amyloid deposits are composed largely of the βA4 peptide, which results from limited proteolysis of the β-amyloid precursor protein (36, 37). While there is no good evidence for transmissibility in Alzheimer disease to experimental animals in contrast to the prion diseases, it is worth questioning whether or not the conversion of an α-helical region in the β-amyloid precursor protein (36) to a β-sheet is a primary event in at least some cases of Alzheimer disease.

The ATR-FTIR method is sensitive to the hydrogen bonding associated with the secondary structure of peptides and proteins, particularly for amide I absorptions at 1700–1600 cm^{-1}. It is a solid-phase method, an essential requirement for

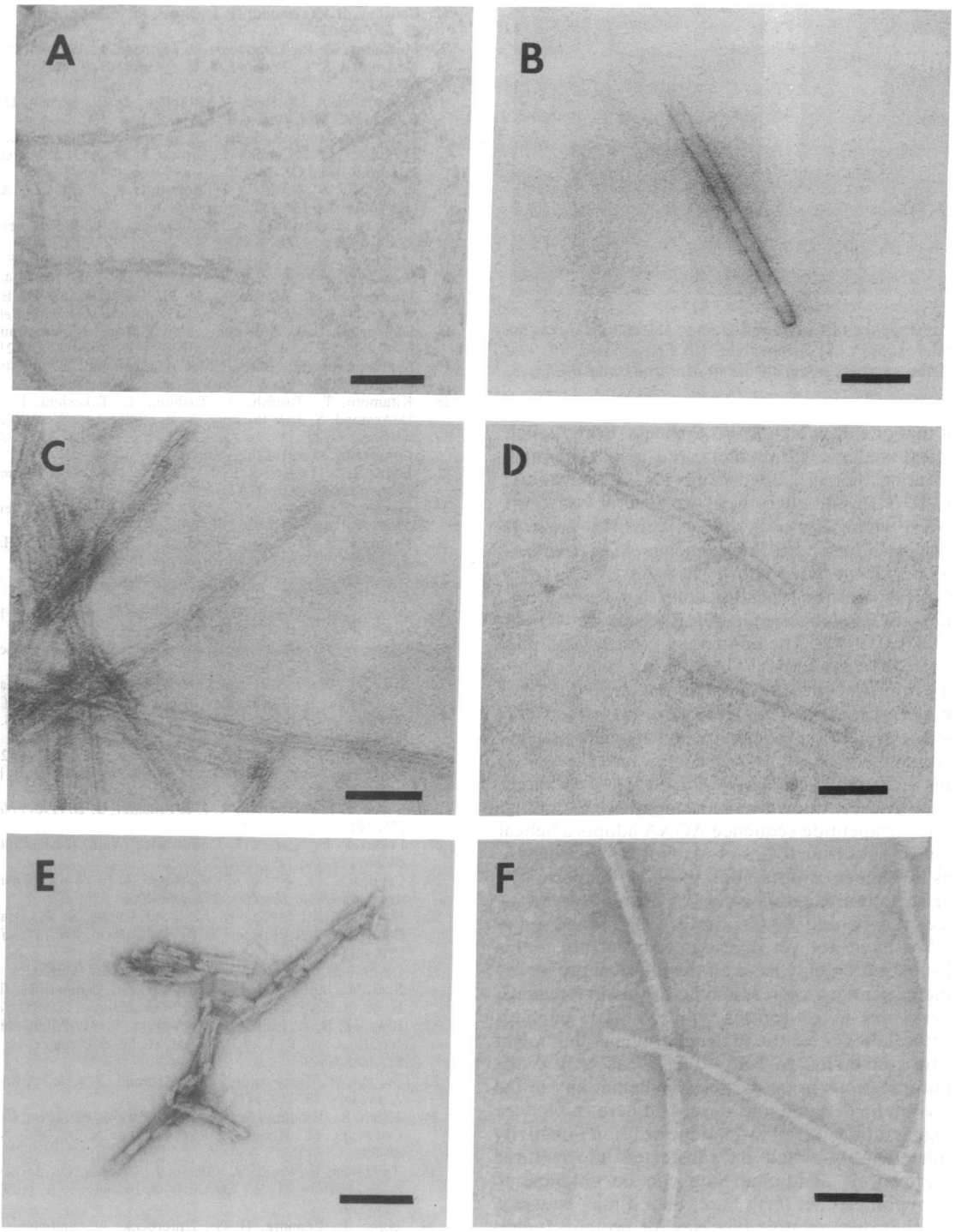

FIG. 3. Electron micrographs of H1 (*A*), SHaPrP-(113–127) (*B*), H3 (*C*), H4 (*D*), prion rods (*E*), and βA4-(1–28) (*F*). The preparation of negatively stained samples is described in *Materials and Methods*. (Bars = 50 nm.)

some of the insoluble peptides included in this study; the peptide is prepared as a thin film on a germanium crystal, which is then hydrated with ^2H_2O. IR has been used to demonstrate the β-sheet structure of various peptide homologues of portions of the βA4 peptide and the effects of pH on the stability of these amyloid structures (28). FTIR studies on the secondary structure of nondenatured PrP 27–30 (19, 20) offer additional experimental data to reconcile the polymerization of PrP 27–30 into amyloid (13) known to be high in β-sheet content (38) and secondary structure predictions based on the primary structure of PrP (18) as well as a possible mechanism for the conversion of PrP^C into PrP^{Sc}.

Prion rods dispersed into detergent/lipid/protein complexes or liposomes retain their infectivity; in fact, prion titers of detergent/lipid/protein complexes or liposomes are enhanced compared with the rods, probably due to increased dispersion (39). When H1 was mixed with phospholipids, it was no longer possible to observe amyloid fibrils by electron microscopy, but ATR-FTIR indicated an increase in the LF-β content. Despite the absence of large polymers when H1 was dispersed into liposomes, we do not know whether the peptide exists in a monomeric or oligomeric state within the liposomes.

There are similarities between the sequence AGAA-AAGA, which is at the core of the amyloid-forming H1 PrP

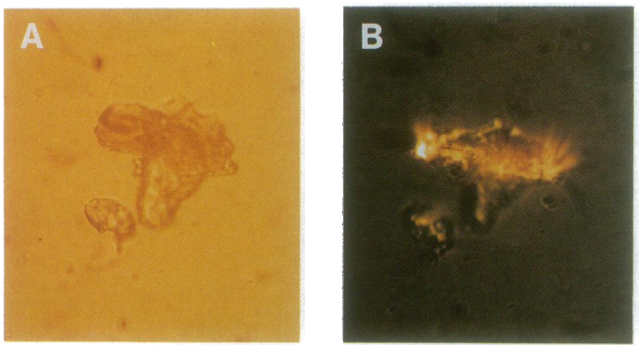

FIG. 4. Birefringence of Congo red-stained H1 viewed by cross-polarization microscopy. (*A*) Bright field. (*B*) Cross-polarized. The preparation of the samples is described in *Materials and Methods*. (×150.)

peptide, and that of silk, which forms β-sheets, even though Garnier–Robson analysis (40) predicts an α-helix. The most common repeating unit in silkworm fibroin, a 108-residue protein, is GAGAGS, although there are several variations based on $(GX)_n$ where X = Ala and/or Ser (41). There is greater homology between the PrP sequence AGAAAAGA-VVGGLGG, which we have shown to form β-sheets and amyloid polymers, and the repeating units in spider fibroin, which contains the sequences AGA_nGGA where $n = 4$, 6, or 7 as well as GGLGG (42). The homeobox protein CUT also has a sequence AGAAAAAAAVGASGG at residues 1880–1894, but it is not known whether this has any structural significance with respect to PrP. Of note is PrP codon 117, which is a site of a mutation genetically linked to Gerstmann–Sträussler–Scheinker disease; with this mutation (Ala → Val) the resulting sequence is AGAAVAGA (43). The three-residue subunit AAA is known to be strongly helix-forming. Curiously, the tetrapeptide sequence AGAA adopts a helical conformation in subtilisin (44) and alcohol dehydrogenase (45) and has a β-sheet conformation in bacteriochlorophyll (46). Similar structural heterogeneity has been observed for the sequences AAAG and AAGA that are also found in the H1 region. We have not yet investigated what effect this amino acid substitution may have on the physical properties of the synthetic peptides corresponding to this PrP region.

In summary, our investigations with synthetic peptides offer a structural model for the molecular events that might feature in the conversion of PrP^C to PrP^{Sc} as well as the replication of infectious prion particles. Whether any of the polymeric synthetic PrP peptides described here can induce neuronal degeneration, PrP^{Sc} formation, or prion infectivity when inoculated into animals or transfected into cultured cells is unknown. If additional data can be obtained to support the hypothesis set forth here, then it may be useful to examine other degenerative diseases for proteins undergoing similar structural changes.

We thank Debra Crumrine for assistance with the electron microscopy and Hana Serban for purification of PrP 27-30. This work was supported by research grants from the National Institutes of Health and American Health Assistance Foundation, as well as by gifts from the Sherman Fairchild Foundation, the Bernard Osher Philanthropic Fund, and the National Medical Enterprises.

1. Prusiner, S. B. (1991) *Science* **252,** 1515–1522.
2. Borchelt, D. R., Scott, M., Taraboulos, A., Stahl, N. & Prusiner, S. B. (1990) *J. Cell Biol.* **110,** 743–752.
3. Caughey, B. & Raymond, G. J. (1991) *J. Biol. Chem.* **266,** 18217–18223.
4. Borchelt, D. R., Taraboulos, A. & Prusiner, S. B. (1992) *J. Biol. Chem.* **267,** 6188–6199.
5. Taraboulos, A., Serban, D. & Prusiner, S. B. (1990) *J. Cell Biol.* **110,** 2117–2132.
6. Caughey, B., Raymond, G. J., Ernst, D. & Race, R. E. (1991) *J. Virol.* **65,** 6597–6603.
7. McKinley, M. P., Taraboulos, A., Kenaga, L., Serban, D., Stieber, A., DeArmond, S. J., Prusiner, S. B. & Gonatas, N. (1991) *Lab. Invest.* **65,** 622–630.
8. Taraboulos, A., Raeber, A., Borchelt, D. R., Serban, D. & Prusiner, S. B. (1992) *Mol. Biol. Cell* **3,** 851–863.
9. Laszlo, L., Lowe, J., Self, T., Kenward, N., Landon, M., McBride, T., Farquhar, C., McConnell, I., Brown, J., Hope, J. & Mayer, R. J. (1992) *J. Pathol.* **166,** 333–341.
10. Prusiner, S. B., Groth, D. F., Bolton, D. C., Kent, S. B. & Hood, L. E. (1984) *Cell* **38,** 127–134.
11. Stahl, N., Baldwin, M. A., Burlingame, A. L. & Prusiner, S. B. (1990) *Biochemistry* **29,** 8879–8884.
12. McKinley, M. P., Meyer, R., Kenaga, L., Rahbar, F., Cotter, R., Serban, A. & Prusiner, S. B. (1991) *J. Virol.* **65,** 1440–1449.
13. Prusiner, S. B., McKinley, M. P., Bowman, K. A., Bolton, D. C., Bendheim, P. E., Groth, D. F. & Glenner, G. G. (1983) *Cell* **35,** 349–358.
14. DeArmond, S. J., McKinley, M. P., Barry, R. A., Braunfeld, M. B., McColloch, J. R. & Prusiner, S. B. (1985) *Cell* **41,** 221–235.
15. Bendheim, P. E., Barry, R. A., DeArmond, S. J., Stites, D. P. & Prusiner, S. B. (1984) *Nature (London)* **310,** 418–421.
16. Kitamoto, T., Tateishi, J., Tashima, I., Takeshita, I., Barry, R. A., DeArmond, S. J. & Prusiner, S. B. (1986) *Ann. Neurol.* **20,** 204–208.
17. Glenner, G. G., Eanes, E. D. & Page, D. L. (1972) *J. Histochem. Cytochem.* **20,** 821–826.
18. Bazan, J. F., Fletterick, R. J., McKinley, M. P. & Prusiner, S. B. (1987) *Protein Engineering* **1,** 125–135.
19. Gasset, M., Baldwin, M. A., Fletterick, R. J. & Prusiner, S. B. (1992) *Proc. Natl. Acad. Sci. USA*, in press.
20. Caughey, B. W., Dong, A., Bhat, K. S., Ernst, D., Hayes, S. F. & Caughey, W. S. (1991) *Biochemistry* **30,** 7672–7680.
21. Goormaghtigh, E., Cabiaux, V. & Ruysschaert, J.-M. (1990) *Eur. J. Biochem.* **193,** 409–420.
22. Gabriel, J.-M., Oesch, B., Kretzschmar, H., Scott, M. & Prusiner, S. B. (1992) *Proc. Natl. Acad. Sci. USA*, in press.
23. Cohen, F. E., Abarbanel, R. M., Kuntz, I. D. & Fletterick, R. J. (1986) *Biochemistry* **25,** 266–275.
24. Stahl, N., Baldwin, M. A., Teplow, D., Hood, L. E., Beavis, R., Chait, B., Gibson, B., Burlingame, A. L. & Prusiner, S. B. (1992) in *Prion Diseases of Humans and Animals*, eds. Prusiner, S. B., Collinge, J., Powell, J. & Anderton, B. (Ellis Horwood, London), in press.
25. Williams, R. C. (1977) *Proc. Natl. Acad. Sci. USA* **74,** 2311–2315.
26. McKinley, M. P., Braunfeld, M. B., Bellinger, C. G. & Prusiner, S. B. (1986) *J. Infect. Dis.* **154,** 110–120.
27. Bazan, J. F., Fletterick, R. J. & Prusiner, S. B. (1987) *Nature (London)* **325,** 581.
28. Fraser, P. E., Nguyen, J. T., Surewicz, W. K. & Kirschner, D. A. (1991) *Biophys. J.* **60,** 1190–1201.
29. Caputo, C. B., Fraser, P. E., Sobel, I. E. & Kirschner, D. A. (1992) *Arch. Biochem. Biophys.* **292,** 199–205.
30. Meyer, R. K., McKinley, M. P., Bowman, K. A., Braunfeld, M. B., Barry, R. A. & Prusiner, S. B. (1986) *Proc. Natl. Acad. Sci. USA* **83,** 2310–2314.
31. Oesch, B., Westaway, D., Wälchli, M., McKinley, M. P., Kent, S. B. H., Aebersold, R., Barry, R. A., Tempst, P., Teplow, D. B., Hood, L. E., Prusiner, S. B. & Weissmann, C. (1985) *Cell* **40,** 735–746.
32. Kascsak, R. J., Rubenstein, R., Merz, P. A., Tonna-DeMasi, M., Fersko, R., Carp, R. I., Wisniewski, H. M. & Diringer, H. (1987) *J. Virol.* **61,** 3688–3693.
33. Serban, D., Taraboulos, A., DeArmond, S. J. & Prusiner, S. B. (1990) *Neurology* **40,** 110–117.
34. Hsiao, K., Dloughy, S., Ghetti, B., Farlow, M., Cass, C., Da Costa, M., Conneally, M., Hodes, M. E. & Prusiner, S. B. (1992) *Nature Genet.* **1,** 68–71.
35. Tagliavini, F., Prelli, F., Ghisto, J., Bugiani, O., Serban, D., Prusiner, S. B., Farlow, M. R., Ghetti, B. & Frangione, B. (1991) *EMBO J.* **10,** 513–519.
36. Kang, J., Lemaire, H.-G., Unterbeck, A., Salbaum, J. M., Masters, C. L., Grzeschik, K.-H., Multhaup, G., Beyreuther, K. & Muller-Hill, B. (1987) *Nature (London)* **325,** 733–736.
37. Glenner, G. G. (1988) *Cell* **52,** 307–308.
38. Glenner, G. G., Eanes, E. D., Bladen, H. A., Linke, R. P. & Termine, J. D. (1974) *J. Histochem. Cytochem.* **22,** 1141–1158.
39. Gabizon, R., McKinley, M. P. & Prusiner, S. B. (1987) *Proc. Natl. Acad. Sci. USA* **84,** 4017–4021.
40. Garnier, J., Osguthorpe, D. J. & Robson, B. (1978) *J. Mol. Biol.* **120,** 97–120.
41. Mita, K., Ichimura, S., Zama, M. & James, T. C. (1988) *J. Mol. Biol.* **203,** 917–925.
42. Xu, M. & Lewis, R. V. (1990) *Proc. Natl. Acad. Sci. USA* **87,** 7120–7124.
43. Doh-ura, K., Tateishi, J., Sasaki, H., Kitamoto, T. & Sakaki, Y. (1989) *Biochem. Biophys. Res. Commun.* **163,** 974–979.
44. McPhalen, C. A. & James, M. N. G. (1988) *Biochemistry* **27,** 6582–6598.
45. Colonna-Cesari, F., Perahia, D. & Karplus, M. (1986) *J. Biol. Chem.* **261,** 15273–15280.
46. Tronrud, D. E., Schmid, M. F. & Matthews, B. W. (1986) *J. Mol. Biol.* **188,** 443–454.